Should "lane formation" occur systematically in driven liquids and colloids?

Jerome Delhommelle

Department of Chemical Engineering, Vanderbilt University, 118 Olin Hall, Nashville, Tennessee 37235-1604, USA
(Received 7 August 2004; revised manuscript received 29 October 2004; published 18 January 2005)

We report on nonequilibrium molecular dynamics simulations of binary mixtures of particles in a color field. Both nonequilibrium molecular dynamics and Brownian dynamics generally assume that the mechanical noise is of thermal origin only and that, at a given temperature, its amplitude remains constant however strong the applied field is. We show that this postulate systematically results in the strong ordering of particles into lanes. By applying a nonequilibrium molecular dynamics method which does not exert any constraint on the noise amplitude, we show that releasing this constraint prevents the systematic "lane formation" from occurring. We observe the onset of density inhomogeneities and jamming instead. This behavior is reminiscent of the shear-thickening regime observed experimentally on colloidal suspensions and in simulations taking into account hydrodynamic interactions.

I. INTRODUCTION

Most natural phenomena occur under nonequilibrium conditions. Many aspects of nonequilibrium systems are still not well understood. For instance, nonequilibrium phase transitions in liquids and colloidal suspensions (subjected to shear or driven by an external field) are far more complex than their equilibrium counterpart. In a three-dimensional crystal, melting occurs through a single first-order transition. When subjected to shear, crystalline colloidal suspensions lose crystalline order in stages, passing through a series of partially ordered intermediate phases before the disordered liquid phase is obtained [1]. Simulation techniques, such as nonequilibrium molecular dynamics (NEMD) and nonequilibrium Brownian dynamics (NEBD), allow a direct observation of the microscopic mechanisms underlying these transitions and should be able to shed light on these phenomena.

An inspection of the literature shows that simulations almost systematically predict the organization of the fluid into highly ordered phases for strong external fields. When a fluid is subjected to high shear rates, a "string phase" forms, as particles align into lines along the flow direction [2–9]. When a binary mixture of "positively and negatively charged" particles [10] is coupled to a strong external field (a system also termed as subjected to a "color field" [11]), "lanes" of particles form, as the system separates into two (or more) blocks of particles of the same color moving in opposite directions [12–16]. A third related phenomenon is the so-called "reentrant freezing" [14,17], which indicates that the equilibrium crystal first melts into a liquid for weak external fields and then rearranges into a liquid crystalline phase for strong external fields. In the liquid crystalline phase, the fluid is organized into layers which move independently from each other at the velocity imposed by the applied shear rate (or, in the case of colored particles, in opposite directions according to the sign with which they couple to the external field). These three phenomena are actually occurrences of a general type of transition, refered to as "lane formation" by Helbing and co-workers in the field of pedestrian dynamics [18]. The quasisystematic occurrence of lane formation in NEBD and NEMD simulations contrasts with the experimental findings. Some experiments report a strong ordering, similar to that obtained in simulations, in colloidal suspensions subjected to high shear rates [19]. However, other experiments indicate that a dramatically different behavior can also be observed. They report the formation of clusters of particles when the fluid is subjected to high shear rates [20,21]. The onset of clustering is accompanied by a steep increase in viscosity (also called shear thickening). We indicate that lane formation results in the opposite behavior—i.e., a sharp decrease in viscosity as the lanes of particles slide past each other with very little friction [22].

The aim of this work is to show that incorrect assumptions, common to conventional NEBD and NEMD methods, result in the systematic occurrence of lane formation. Helbing *et al.* [18] indicate that lane formation occurs at a small noise-to-field ratio. Both NEBD and NEMD methods rely on the assumption that the amplitude of mechanical noise is constant however strong the external field is. In NEBD methods, the amplitude of random forces, describing the effect of the solvent on colloidal particles, is a function of the friction coefficient and of the temperature. Similarly, in NEMD methods, the amplitude of velocity fluctuations is generally fixed through a kinetic thermostat, which accounts for the dissipation of heat and allows the system to reach a steady state. At a given temperature, the noise amplitude is kept constant in both methods, regardless of the intensity of the field. Increasing the field intensity leads to lower noise-to-field ratio and inevitably results in lane formation for strong enough fields.

Conventional NEBD and NEMD methods postulate that mechanical noise can only be of thermal origin. However, mechanical noise is partly of hydrodynamic origin. While hydrodynamic effects are certainly negligible for low fields, the hydrodynamic contribution to the mechanical noise becomes significant for strong fields, in the very range of fields for which lane formation is observed. Several studies support the significance of these hydrodynamic effects. By applying a stability analysis to a simple liquid subjected to shear, McWhirter [23] showed that, at high shear rates, secondary flow profiles develop along the flow direction and in directions perpendicular to the flow. Moreover, in NEBD calcula-

tions, adding the hydrodynamic contribution enables us to recover the experimentally observed shear-thickening behavior instead of the string phase [24,25]. Similarly, in NEMD calculations, using a configurational thermostat (i.e., a thermostat which does not fix the amplitude of velocity fluctuations) enables us to observe the onset of shear thickening [22,26]. At this point, it is useful to note that we expect non-Newtonian effects to arise. Systems studied by simulation consist typically of 1000 particles in periodic boundary conditions. This imposes a lower limit on the wave vector describing collective motion and prevents large-scale instabilities. The Reynolds number remains therefore low even for extremely high shear rates, and one observes non-Newtonian rather than turbulent behavior.

In order to characterize the relationship between the assumption of constant noise amplitude and the phenomenon of lane formation, we perform NEMD simulations with a kinetic thermostat (a method assuming that all mechanical noise is thermal) or a configurational thermostat (a method making no such assumption). We study binary mixtures of two-dimensional (2D) and 3D colored particles driven by an external field. In the next section, we show that NEMD, when performed with a kinetic temperature thermostat, and NEBD simulations [12–15] yield very similar results regarding lane formation for 2D systems. In particular, we obtain (i) for all densities, a systematic lane formation when the applied field exceeds a threshold value [12–15], (ii) reentrant freezing at high values for the external field [14], and (iii) a reentrance effect for a fixed high driving field as the system undergoes a sequence of states no lane→lanes→no lane with increasing density [15]. The agreement between the results obtained with the two methods shows that lane formation is induced by the assumption of constant noise amplitude, common to both methods. This also demonstrates that lane formation is not related to any other effect (e.g., to the presence of the solvent in NEBD methods). We further assess this result by showing that releasing the constraint of constant mechanical noise prevents lane formation. This is achieved by performing NEMD calculations using using a configurational thermostat [22,26–31]. Instead of lane formation, we observe the onset of density inhomogeneities and of jamming, a behavior similar to that observed in the shear-thickening regime for a colloidal suspension [20,21] or a simple fluid [22,26] undergoing shear flow. We then extend our study to 3D systems and examine the behavior of the system if the noise amplitude is assumed to be constant in all directions, in one direction (either parallel or perpendicular to the field), or if the noise amplitude is not fixed. We find that lane formation only occurs if the noise amplitude is assumed to be constant in all directions. Using any other method, we observe jamming.

II. SIMULATION METHOD

We study 2D systems of $N=896$ soft disks with the pair interaction potential $\phi(r)=\varepsilon(\sigma/r)^{12}$. In all simulations, we use a reduced system of units, where the unit of mass is the mass of the particle m, the unit of energy is the characteristic energy ε of the pair potential, and the unit of length is the

particle exclusion diameter σ. Simulations were all carried out at a reduced temperature $T=1$ and for various reduced number densities $n=1.03$ (approximately at the solid-liquid coexistence [32–35]), 0.92, 0.75, 0.6, and 0.5. Some simulations were also run on 3D systems of $N=1000$ Weeks-Chandler-Andersen (WCA) particles with the pair interaction potential $\phi(r)=\varepsilon(1-4[(\sigma/r)^6-(\sigma/r)^{12}])$ for $r\leqslant 2^{1/6}\sigma$ and 0 otherwise. The thermodynamic-state point chosen for the 3D system ($n=0.84$, $T=0.722$ in reduced units with respect to the WCA parameters) corresponds approximately to the triple point for the Lennard-Jones fluid. In the remainder of the paper, all results will be given in reduced units.

We use Newton's equations of motion supplemented with a thermostatting mechanism. The purpose of the thermostat is to account for the dissipation of heat and to allow the simulated system to reach a steady state. Similarly to what occurs in colloidal suspensions where the solvent plays the role of a heat bath, heat is removed homogeneously by the thermostat.

First, we use a Gaussian isokinetic thermostat which fixes the kinetic energy of the system and the temperature given by the equipartition principle as

$$T = \frac{\langle \sum_{i=1}^{N} m\mathbf{v_i}^2 \rangle}{2Nk_B}. \tag{1}$$

Another possible choice is to define a kinetic temperature relative to the flow, using the momenta relative to the flow velocity of each type of particles. We showed in previous work on molten NaCl in an electric field [36] that both types of expressions yielded similar results. The equations of motion are

$$\dot{\mathbf{r}}_i = \frac{\mathbf{p}_i}{m},$$

$$\dot{\mathbf{p}}_i = \mathbf{F}_i + \epsilon_i F^{ext}\mathbf{e}_x - \xi\mathbf{p}_i, \tag{2}$$

where $\mathbf{p}_i$ is the momentum of particle i, $\mathbf{F}_i$ the Newtonian force exerted on i, and $\epsilon_i=\pm 1$ is the sign whith wich particle i couples with the applied external field $F^{ext}\mathbf{e}_x$ ($\mathbf{e}_x$ is an unit vector along the x axis). ξ is the thermostatting multiplier given by Gauss' principle of least constraint:

$$\xi = \frac{\sum_{i=1}^{N}(\mathbf{F}_i + \epsilon_i F^{ext}\mathbf{e}_x)\cdot\mathbf{p}_i}{\sum_{i=1}^{N}\mathbf{p}_i\cdot\mathbf{p}_i}. \tag{3}$$

This set of equations of motion obviously limits the amplitude of velocity fluctuations and hence of mechanical noise.

Second, we use a configurational thermostat which fixes a configurational expression for the temperature [37,38]. This expression allows the calculation of temperature solely from configurational quantities, such as first and second spatial derivatives of the interaction energy. This thermostat exerts absolutely no constraint on the velocity fluctuations or on the noise amplitude. The configurational expression for the temperature is

$$\frac{1}{k_B T} = \frac{\left\langle \sum_{i=1}^{N} \frac{\partial^2 \Phi_0}{\partial \mathbf{r}_i^2} \right\rangle}{\left\langle \sum_{i=1}^{N} \left(\frac{\partial \Phi_0}{\partial \mathbf{r}_i} \right)^2 \right\rangle}, \quad (4)$$

where Φ_0 is the potential energy of the system and $\mathbf{r}_i$ the position of particle i. The configurationally thermostatted equations of motions are [22,26–31]

$$\dot{\mathbf{r}}_i = \frac{\mathbf{p}_i}{m} + \frac{s}{T} \frac{\partial T_{conf}}{\partial \mathbf{r}_i},$$

$$\dot{\mathbf{p}}_i = \mathbf{F}_i + \epsilon_i F^{ext} \mathbf{e}_x,$$

$$\dot{s} = -Q \frac{(T_{conf} - T)}{T}, \quad (5)$$

where T is the imposed temperature while T_{conf} is the value given by Eq. (4) [Q is a damping constant set to $10(m\sigma^4/\varepsilon)$].

In equilibrium, the kinetic and configurational expressions for the temperature are equivalent. They can be derived from the thermodynamic definition for the temperature as the inverse rate of change of entropy with internal energy at constant volume, using Gibbs microscopic expression for entropy. Therefore, in equilibrium, using a kinetic thermostat is equivalent to using a configurational thermostat, provided that the equations of motion are integrated with accuracy. This may not be true when large time steps are used. In that case, more sophisticated integration schemes may be needed [39,40]. However, as noted by Soddemann and co-workers [41], the choice of a rather hard potential to describe the particle interactions (as for the soft disks or WCA particles studied in this work) leads us to use a small time step in order to simply achieve numerical stability. For such a small time step, the numerical solution is usually quite accurate. Extending both kinetic and configurational definitions to systems out of equilibrium implies the approximation that the assumption of local equilibrium is valid. This is assumed in both types of temperature definitions when used out of equilibrium; otherwise, temperature would not be a well-defined quantity. However, the configurational expression is free from errors stemming from an incorrect estimate of which part of the actual particle velocities should be associated to thermal fluctuations, and therefore can be considered as "more correct."

The equations of motion were integrated using a fourth-order Gear predictor-corrector algorithm with a time step $\tau = 0.001$, except at the highest fields for which a smaller time step had to be used. Before applying any external field, we created for each density an initial configuration by running an equilibrium simulation at the desired temperature and density. We then attribute at random a "plus" charge to half of the particles of the system and a "minus" charge to the other half. Two runs of 5000 time units are then carried out for each value of the field. We found that the system had always reached a steady state at the end of the first run.

Properties of interest are averaged over the second run of 5000 time units. The final configuration obtained at the end of the second run is used afterwards as the starting configuration for the runs at the next larger value for the field.

We monitor the variations of the order parameter ϕ to detect the onset of lane formation. ϕ is defined as $\phi = \langle \Sigma_{i=1}^{N} \phi_i / N \rangle$ where ϕ_i is equal to 1 for a given particle i if the distance, along the x axis, to all particles j of the opposite charge is larger than the distance between two nearest neighbors (i.e., such that $|x_i - x_j| > n^{-1/2}$ in 2D and $|x_i - x_j| > n^{-1/3}$ in 3D) and equal to 0 otherwise. If particles of the same color align along the x direction (i.e., the direction of the field), ϕ will be equal to 1. On the contrary, ϕ vanishes in a randomly mixed configuration. In the specific case of the 2D system at $n = 1.03$, which is crystalline at equilibrium, we monitor the variations of another order parameter noted as ψ_6, which is the global six-fold bond-orientational parameters commonly used to measure the amount of triangular ordering of the system as a whole (see, e.g., [31]). It is defined as

$$\psi_6 = \frac{1}{N} \sum_{j=1}^{N} \phi_{6j}. \quad (6)$$

The local sixfold bond-orientational order parameter ϕ_{6j} for a particle j is defined by

$$\phi_{6j} = \frac{1}{n_j} \sum_{k=1}^{n_j} e^{6i\theta_{jk}}, \quad (7)$$

where n_j is the number of nearest neighbors of particle j, and θ_{jk} is the angle of the "bond" between particle j and its kth nearest neighbor, measured relatively to an arbitrary fixed axis. The set of nearest neighbors is determined from the Voronoi construction [42].

III. BEHAVIOR AT CONSTANT MECHANICAL NOISE

We first present the results obtained at constant mechanical noise for 2D systems subjected to a color field. Simulations were carried out with a kinetic temperature thermostat for $n = 1.03$ (in equilibrium, this system is a 2D crystal). The variations of the potential energy and of the potential part of pressure are plotted against the applied field in Fig. 1. The variations of the configurational temperature of the system and of the two order parameters ϕ and ψ_6 are shown in Fig. 2. Both plots show four different stages in the response of the system for the range of fields investigated. The first stage takes place for low values of the field ($F^{ext} < 1.25$). The system is still crystalline, as shown by the fact that ψ_6 remains very close to its equilibrium value of 0.75 (because of thermal motion, ψ_6 is not equal to 1 at equilibrium) [31]. We monitor slight increases in both pressure and potential energy with increasing field as the crystal gets more and more strained. In this regime, there is no inaccuracy attached to the determination of the kinetic temperature since the system does not flow and the configurational and the kinetic expressions for the temperature take the same value (within statistical errors). For $F^{ext} = 1.25$, we observe a sharp drop for all properties (except for ϕ) which corresponds to melting of the
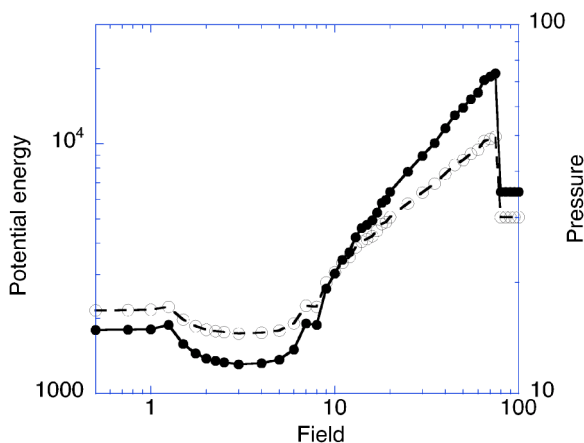
FIG. 1. Potential energy (solid circles) and potential part of pressure (open circles) against the applied field.

strained crystal. We then observe the second stage for $1.25 \leqslant F^{ext} \leqslant 8$. This second stage is characterized by a steady decrease in potential energy, pressure, and configurational temperature with increasing field until all properties reach a plateau. The decrease in the various properties concomitantly occurs with a gradual lane formation as indicated by the steady increase of ϕ (maximum of 0.8 at $F^{ext}=6$) and in ψ_6 (maximum of 0.59 at $F^{ext}=4$). We also observe a plateau for the two order parameters for $3 \leqslant F^{ext} \leqslant 8$. In this range of fields, the system experiences the so-called reentrant freezing. The system is actually composed of two demixed crystalline lanes sliding against each other (the flow velocity profile is constant throughout each lane and the two lanes move at the same velocity in opposite directions) as previously observed in NEBD simulations [13]. There is a strong correlation between the onset of lane formation and the decrease in configurational temperature. One would expect that, in a nonequilibrium system, the unthermostatted degrees of freedom to heat up. Hence, in the steady state, the configurational temperature should be higher than the imposed value for the kinetic temperature. When the system is demixed into two lanes, the configurational temperature reaches a mini-

mum of 0.04 ($F^{ext}=6$), considerably less than the imposed value of 1 for the kinetic temperature. Any instability or any difference between the actual steady-state flow profile and the assumed flow profile in Eq. (1) is interpreted as "mechanical noise" by the simulation algorithm. Since the total noise amplitude is fixed, the method results in attenuated thermal fluctuations [30]. The actual temperature within the fluid is therefore much lower than the imposed value of 1. This is demonstrated by the very low value taken by the configurational temperature (only 4% of the imposed value for the kinetic temperature). The third stage takes place for $3 \leqslant F^{ext} \leqslant 80$. It is associated with a steady increase in potential energy, pressure, and configurational temperature and a steady decrease in both order parameters with increasing field. Given that the interface between the two lanes moving in opposite directions is not smooth (as can be seen in Fig. 3), there is more and more friction at the interface as the applied field is increased. This causes the two lanes to break down in smaller entities. These entities (or domains) are composed of particles of the same charge, which collide with each other, giving rise to jamming. We emphasize that it is a particular type of jamming since ϕ always remains very large (this point will be discussed in more detail in the following sections). The final stage takes place for $F^{ext}>80$ as the system demixes again in several lanes of identical particles, each lane moving along the x axis at the velocity imposed by the thermostat ($v=\sqrt{2k_BT/m}$). In this regime, the component of the velocity of a particle along the y axis is equal to 0 and the lanes slide against each other. There is absolutely no friction for this system as indicated by the constant value obtained for all properties for all values of the field greater than 80. The state of the system has become independent from the value of the applied field.

The mechanism described above for $n=1.03$ is observed for all densities larger than 0.6 and is summed up in the snapshots (obtained for a density of 0.75) presented in Fig. 3. Note that the high-field regime observed for $n=0.75$ (starting for $F^{ext}>55$) slightly differs from the one observed at $n=1.03$. There are actually a few particles trapped in lanes of the opposite sign, resulting in some friction and very slow increases in pressure and potential energy with increasing field. This has no consequence on the stability of the lanes as the order parameter ϕ remains equal to 0.5 throughout this regime ($55<F^{ext}<100$). We add that for the two smaller density studied here ($n=0.5$ and $n=0.6$), the fluid demixes directly into several lanes at low fields ($F^{ext}=10$ and 20, respectively). In agreement with previous NEBD studies, lane formation occurs for any state point provided that the field is strong enough. We sum up the results obtained with a kinetic thermostat for the variations of the order parameter with the applied field and with the density of the system under study in Fig. 4, which shows that the phenomenon of reentrance, recently obtained in NEBD simulations [15], can also be observed in NEMD simulations. For a given value for the field e.g., $F^{ext}=1.75$, lane formation is only observed for an intermediate range of densities ($\phi>0.7$ for $n=0.75$ and 0.92). It takes place neither at low densities ($\phi=0.34$ for $n=0.5$) nor at high densities ($\phi=0.36$ for $n=1.03$).
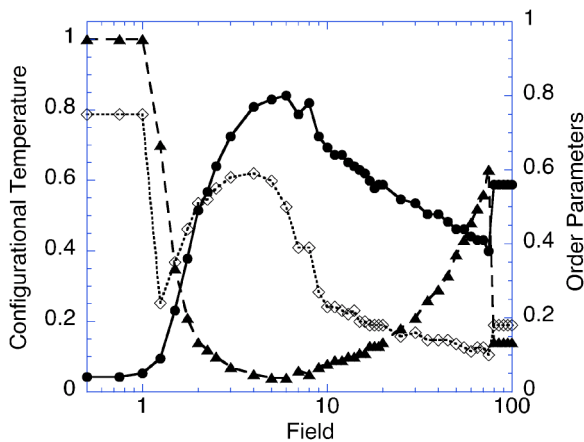

FIG. 2. Configurational temperature (solid triangles), order parameter ϕ (solid circles), and six-fold bond-orientational order parameter ψ_6 (open diamonds) against the applied field.
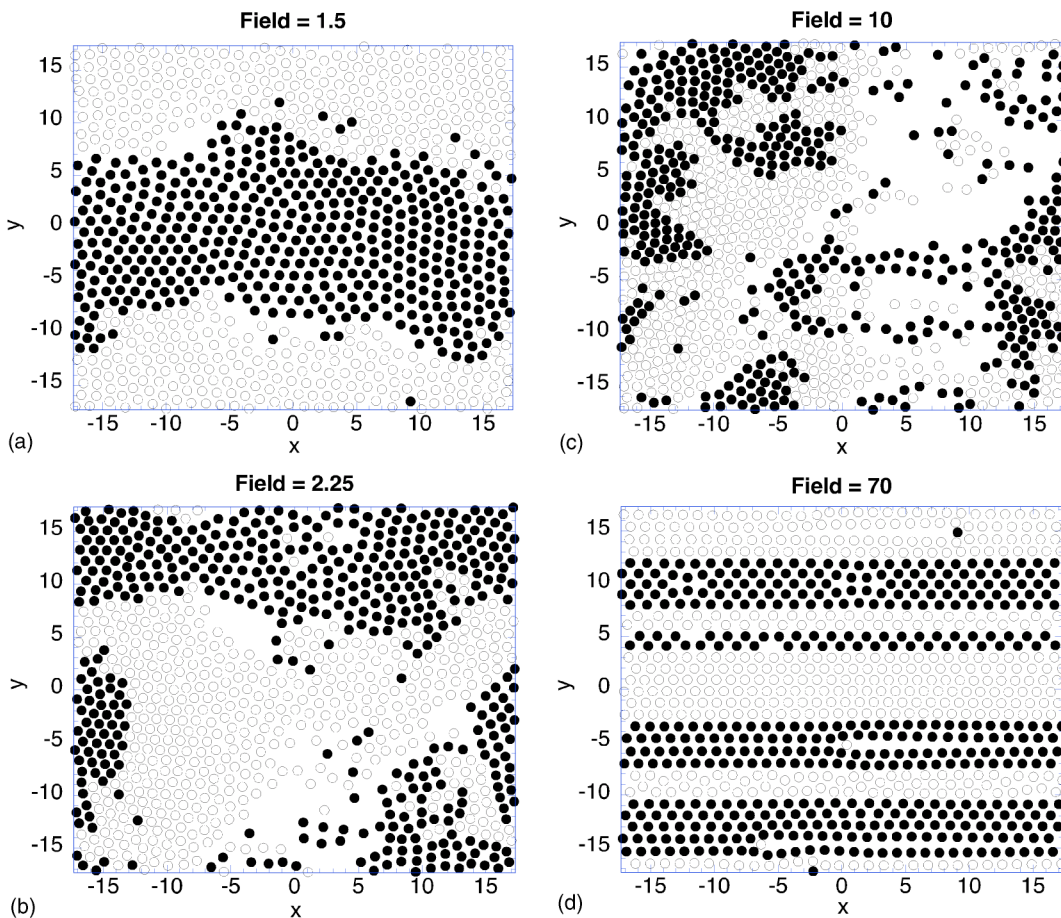
FIG. 3. Mechanism observed at constant kinetic temperature for a density of 0.75: organization in two lanes (field=1.5), lanes start to break up (field=2.25), lanes are completely broken up (field=10), and reorganization in multiple lanes (field=70). Same legend as in Fig. 5.

IV. BEHAVIOR AT CONSTANT CONFIGURATIONAL TEMPERATURE

We now study 2D systems in a color field by NEMD with a configurational thermostat. Figure 5 shows the variations of the potential energy and of the potential part of pressure with the applied field. The variations of the kinetic temperature of the system and of the order parameters ϕ and ψ_6 with the field are plotted in Fig. 6. Two regimes can be identified from Fig. 5. First, pressure and potential energy steadily increase with increasing field for $0 < F^{ext} < 1$. In this regime, the value of the order parameter ψ_6 remains close to its equilibrium
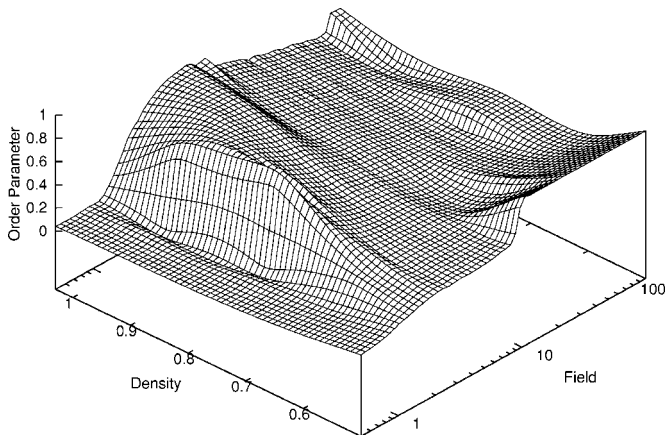

FIG. 4. Variation of the order parameter ϕ with the applied field and the density of the system.
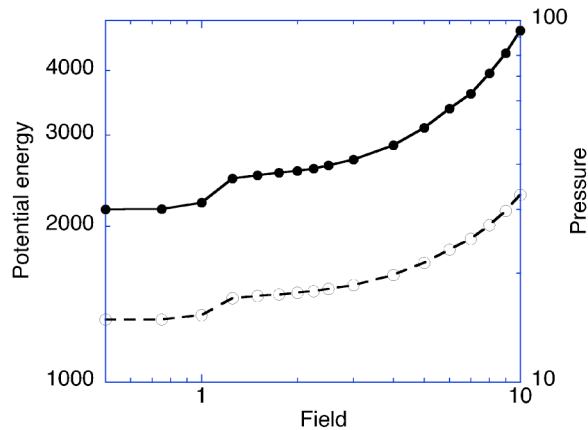

FIG. 5. Potential energy (solid circles) and pressure (open circles) against the applied field.
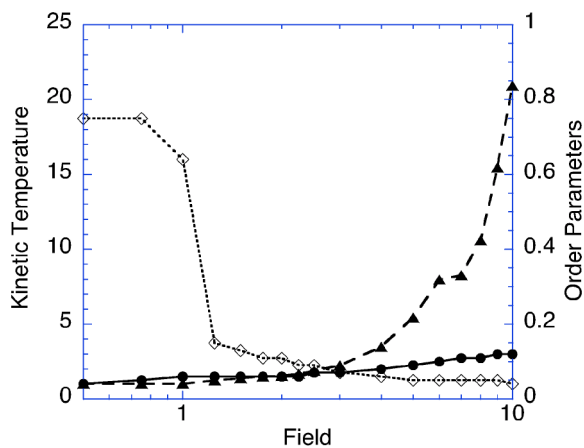
FIG. 6. Kinetic temperature (solid triangles), order parameter ϕ (solid circles), and six-fold bond-orientational order parameter ψ_6 (open diamonds) against the applied field.

value of 0.75 and the system retains its crystalline order. As expected, the kinetic temperature stays equal to 1.0—the value fixed by the configurational thermostat—in this regime. There is then a jump in both pressure and potential energy associated with a sharp decrease in ψ_6 (see Fig. 6) as

the crystal melts into a liquid when the applied field F^{ext} exceeds 1.0. The second regime takes place afterwards for $F^{ext} \geqslant 1.25$. It is characterized by a steady increase in pressure and potential energy with the field and by a gradual loss of crystalline order as indicated by the steady decrease of ψ_6. We note a steep increase in the kinetic temperature evaluated using Eq. (1) as the unthermosttated degrees of freedom heat up and reach, in the steady state, a larger value than the imposed value for the configurational temperature. For the range of fields investigated ($F^{ext} \leqslant 10$), the system remains in a liquid state. We do not observe any lane formation. The relevant order parameter ϕ slowly increases and reaches a maximum value of 0.12 for the two highest fields. As we saw in the previous section, lane formation is associated with an order parameter ϕ of about 0.8 (this value was reached for $F^{ext} = 6$—a value well within the range of fields investigated here). This value of ϕ indicates that there is a small charge separation effect but no lane formation. On the contrary, increasing the strength of the applied field induces density inhomogeneities and jamming (Fig. 7), associated with large values for the potential energy and pressure as well as large fluctuations in the pressure fluctuations. This is reminiscent of our findings on simple fluids undergoing shear flow: using a configurational thermostat, we observed the onset of density inhomogeneities, of jamming, and of large pressure fluc-
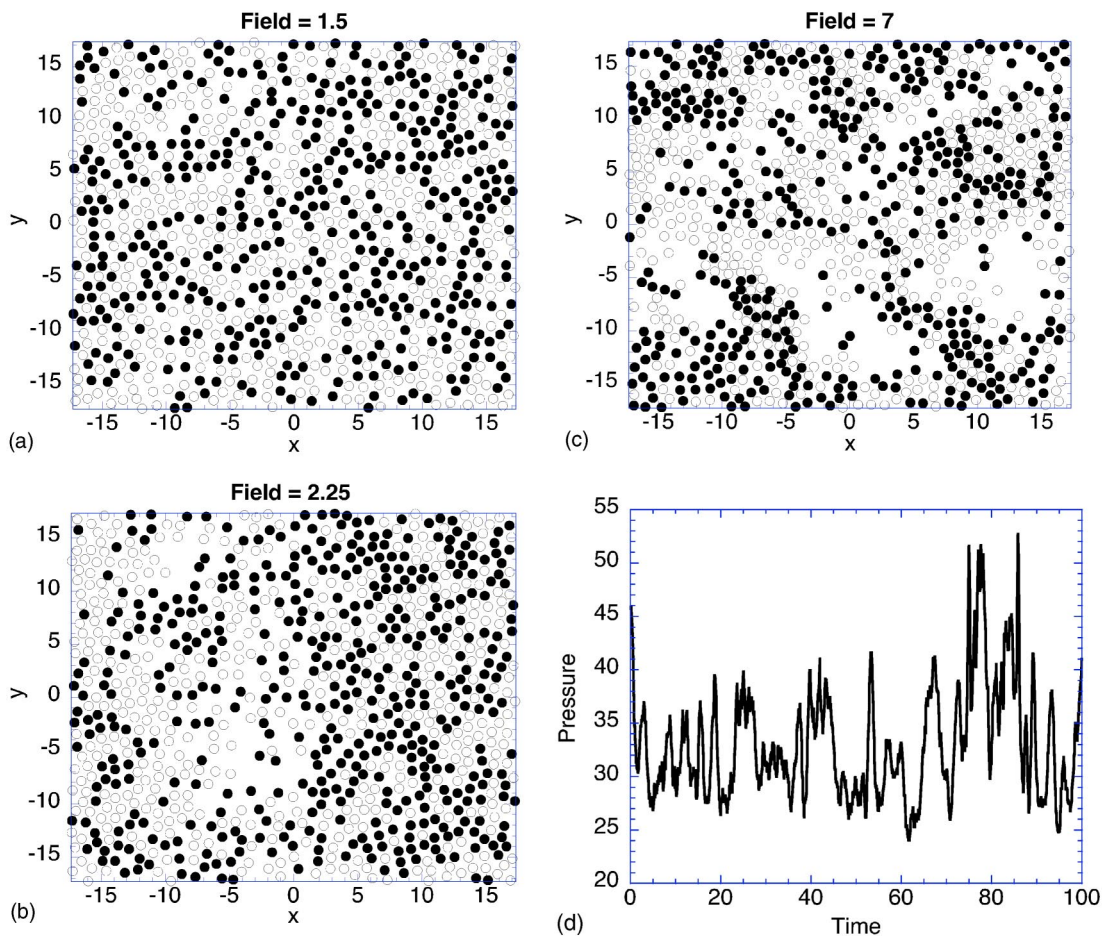

FIG. 7. Mechanism leading to inhomogeneities and jamming with an increasing applied field ($d=0.75$, constant configurational temperature).
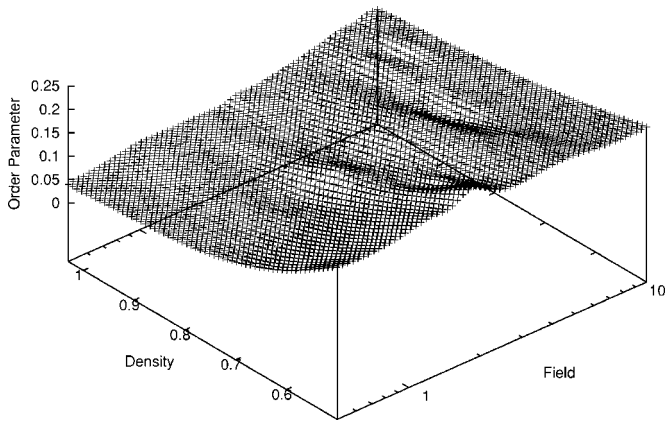
FIG. 8. Variation of the order parameter ϕ with the applied field and the density of the system.

tuations at high shear rates, giving rise to shear thickening [26]. We emphasize that the type of jamming observed with a configurational thermostat strongly differs from that observed in Fig. 3 for intermediate values for the field. Indeed, when a configurational thermostat is used, jamming occurs in well-mixed fluids with low values for ϕ. Clusters are composed of both "positive and negative charge" particles and there are no large domains of identical particles. We finally plot in Fig. 8 the variations of the order parameter as a function of the applied field and of the density of the system. The order parameter ϕ takes very low values for all densities and values for the field and always remains below 0.24. We do not observe any lane formation in any simulation carried out with a configurational thermostat.

V. COMPARISON BETWEEN THE TWO SCENARIOS

We now move on to the study of a binary mixture of 3D colored WCA particles at $n=0.84$ and $T=0.722$. We use four different types of thermostat: (i) a Gaussian kinetic thermostat fixing the total kinetic energy, (ii) a configurational thermostat, (iii) a Gaussian kinetic thermostat fixing the kinetic energy along the flow direction, and (iv) a Gaussian kinetic thermostat fixing the kinetic energy along one of the directions perpendicular to the flow. The potential part of pressure and the order parameter ϕ are plotted against the field in Fig. 9, which shows that only one method (fixing the total kinetic energy) yields to lane formation. The amplitude of mechanical noise must therefore be kept constant in directions both along and perpendicular to the flow to allow for lane formation. Fixing the kinetic energy along the flow direction only amounts to limiting the "color" current and thus delay the onset of instabilities and jamming. The system partially demixes as indicated by a dip in pressure and a maximum value of 0.36 for ϕ. However, there is no lane formation. Instabilities appear for larger fields ($F^{ext} \gtrsim 5$), resulting in an increase in pressure and a decrease in ϕ. Fixing the kinetic energy along a direction perpendicular to the flow or fixing the configurational temperature give qualitatively similar results. In both cases, ϕ increases and then reaches a plateau for $F^{ext} \gtrsim 4$ while the pressure increases steeply as jamming sets in.
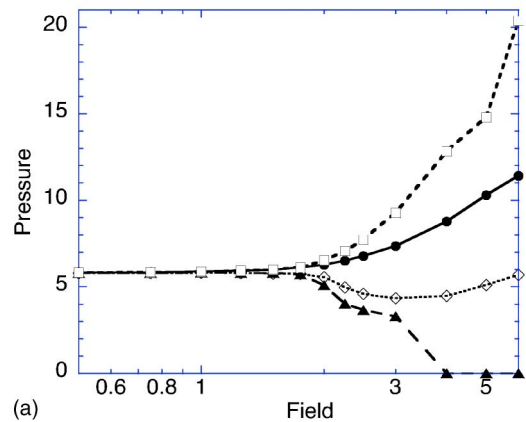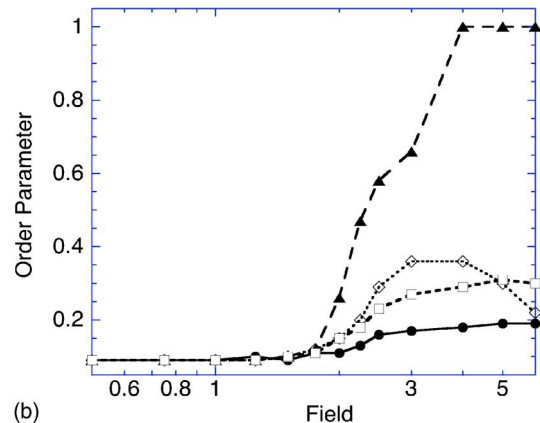
FIG. 9. Variation of (a) pressure and (b) ϕ with the applied field for a WCA fluid using various thermostats fixing either the total kinetic energy (solid triangles), the kinetic energy along the flow direction (open diamonds), the kinetic energy along one of the directions perpendicular to the flow direction (open squares), or the configurational temperature (solid circles).

Fixing the noise amplitude along a direction perpendicular to the flow (i.e., partially frustrating the system) results in a slightly larger value for ϕ in the plateau (0.30 against 0.19). However, in both cases, the fluid remains mixed. The agreement obtained between the last two types of simulation shows that lane formation is an artefact arising from the assumption of constant noise amplitude. It also shows that jamming will be observed in strongly driven liquids and colloidal suspensions.

We finally highlight the similarities between systems subjected to a color field and simple fluids subjected to shear. We extend the results obtained in our previous work (details of the numerical procedure are given in Ref. [22]) to very high shear rates (up to 40). We plot the corresponding flow curve in Fig. 10. As observed for particles in a color field, using NEMD together with a configurational thermostat leads to density inhomogeneities, clustering and jamming. This translates into an increase in the shear viscosity for shear rates larger than 7 and to the onset of shear thickening. On the contrary, when a kinetic thermostat is used, lane formation takes place for shear rates larger than 1.5. When lane formation occurs, we observe a sharp drop in shear viscosity which is consistent with our physical intuition since lanes of
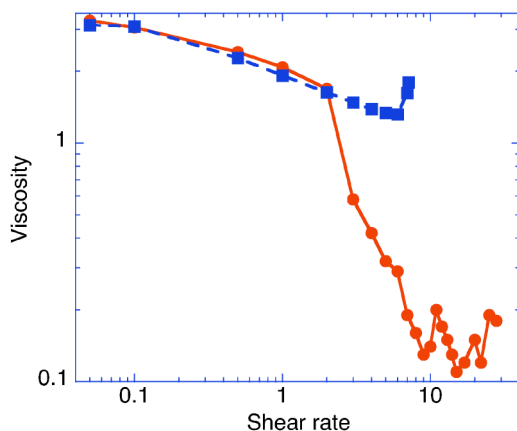
FIG. 10. Viscosity against shear rate for a WCA fluid using a kinetic thermostat (solid circles) or a configurational thermostat.

particles sliding past each other should result in a very low value for the viscosity. For larger shear rates than 10, the viscosity exhibits nonmonotonic variations with shear rate, a regime which has been sometimes interpreted as an "indication for shear thickening" [43,44]. However, this effect does not correspond to the phenomenon observed experimentally (also observed using Stokesian dynamics [24,25] or NEMD with a configurational thermostat [26]). The postulate of con-

stant noise amplitude forces the system to remain organized into strings along the flow direction. As shown in Fig. 11, the organization of the fluid into lanes becomes more and more pronounced as the shear rate is increased. The nonmonotonic variations in shear viscosity are actually due to collisions between particles and jamming within the same lane. Density inhomogeneities and jamming in all directions of space, which would correspond to the actual shear-thickening phenomenon, do not happen since they are frustrated by the use of a kinetic thermostat. This phenomenon is similar to the type of jamming observed in a color field when a kinetic thermostat is used (see Fig. 3 for $F^{ext}=10$). In the latter, jamming occurs in a "frustrated" 2D fluid—i.e., a fluid which remains significantly demixed ($\phi=0.56$) for all values for the field.

VI. CONCLUSIONS

In this work, we showed that using conventional simulations technique (either NEBD or NEMD with a kinetic thermostat) systematically results lane formation in liquids subjected to strong external fields. The similarity between NEBD and NEMD results stems from an incorrect assumption common to both methods. Both methods postulate that, for a given system (i.e., at fixed friction coefficient in
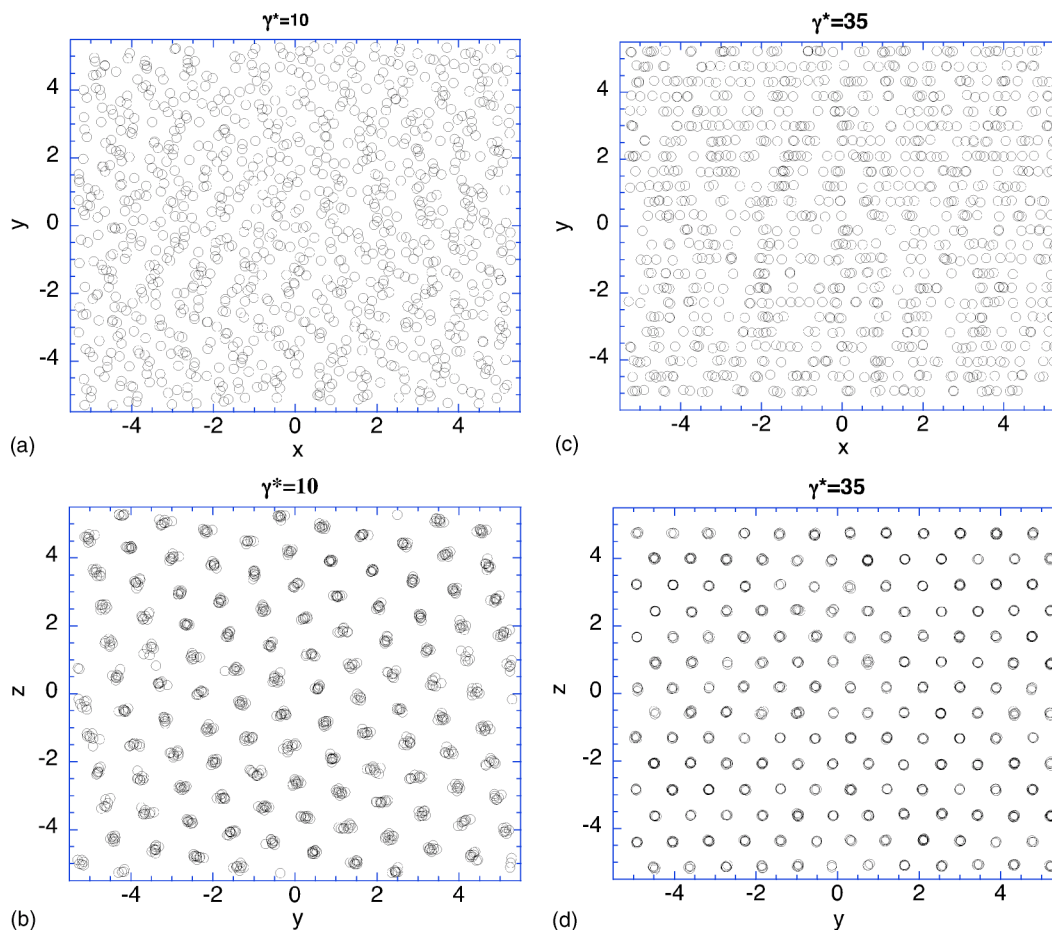

FIG. 11. Snapshots of a WCA fluid undergoing shear flow in the x-y and y-z planes for a shear rate of 10 (top) and 35 (bottom).

NEBD), the amplitude of velocity fluctuations is a function of temperature only. However, the velocity fluctuations are not all of thermal origin. They are also partly of hydrodynamic origin and reflect the onset of local flows. As the intensity of the field increases, local flows develop and the hydrodynamic contribution to the velocity fluctuations becomes more and more significant. The error made in NEBD and in NEMD using a a kinetic thermostat dramatically increases with the field. It eventually leads to lane formation, as shown in this work for both 2D and 3D systems. Two criteria have allowed us to determine that this systematic lane formation was artificial. First, the sharp drop exhibited by the configurational temperature, simultaneously to the onset of lane formation at high external fields indicated that the kinetic thermostat overly dampened thermal fluctuations. This means that the actual temperature is much lower than the one fixed by the thermostat. Second, we showed that lane formation can only be obtained in a very restrictive case. Results on 3D systems demonstrate that the mechanical noise amplitude has to be fixed in all directions of space to allow for lane formation.

An obvious solution to this problem would consist in taking into account the field dependence of velocity fluctuations. This can be done by adding a hydrodynamic contribution in NEBD or by devising a profile unbiased thermostat (PUT) [11] in NEMD, which only acts on the thermal part of the velocity fluctuations. Such a thermostat fixes the kinetic energy relative to the flow, obtained by subtracting the exact flow velocity to the absolute velocities of the particles. An accurate determination of the flow velocity implies averaging the particle velocities over some period of time or some region of space. Unfortunately, the flow velocity is both spatially and temporally dependent in strong fields, and the scales on which it changes are comparable to thermal fluctuations in time and to atomic distances. It is therefore impossible to completely separate the thermal from the hydrodynamic contributions. The determination of the flow velocity will always suffer from some inaccuracy. The use of the corresponding PUT will be fraught with similar (though less severe) deficiences to that of a conventional kinetic thermostat. Indeed, different implementations of PUT have led to contradictory conclusions: while some studies report a lane formation [4,5,8], others show that using a PUT destabilized the so-called string phase [45–47].

In this work, we showed that using a configurational thermostat is a satisfactory way to deal with this issue. The configurational thermostat is free from these artifacts since it does not require making any assumptions about the flow velocity. It therefore constitutes a much safer way to account

for heat dissipation in nonequilibrium systems, particularly when the flow profile is *a priori* unknown (e.g., in inhomogeneous systems [30,31] or in non-Newtonian fluids [48]). Another means of avoiding such errors is to employ local momentum-conserving thermostats, such as dissipative particle dynamics. In this case, the friction does not dampen the absolute velocities of the particles, but rather the velocity differences between nearby particles [41]. It would be interesting to use the scheme proposed by Soddemann *et al.* to further assess the results obtained in this work.

Disorder→order transitions do exist in strongly driven nonequilibrium systems. For instance, experimental studies report that colloidal suspensions order when subjected to oscillatory shear [19]. We previously reported such an ordering in NEMD simulations (using a configurational thermostat) of a simple liquid undergoing oscillatory shear flow [48]. However, the assumptions made in conventional simulations "frustrate" the system and systematically lead to lane formation. In some cases, ordering is a genuine phenomenon. Using conventional methods will give rise to lane formation and will preempt or obscure the mechanism by which ordering takes place. In other cases, a strong external field results in density inhomogeneities and large pressure fluctuations [20,21]. Conventional NEBD and NEMD techniques are unable to account for this phenomenon, unlike the method presented in this work.

We emphasize that the results presented in this work have many possible applications—e.g., on the mechanism for conductivity in ionic liquids and on ion transport in biological applications or if particles with different masses are subjected to a gravitational field. Of course, the situation described in this work does not exactly correspond to what happens in ionic fluids. Indeed, there are no "colored" interactions between the particles subjected to a color field while there are Coulombic interactions between ions. This makes lane formation impossible in a real ionic fluid. We did not observe this phenomenon in previous work on molten NaCl subjected to shear [49] or to an electric field [36,50]. However, even if lane formation does not occur, using a method which arbitrarily fixes the noise amplitude can greatly affect transport properties. As shown in previous work [36], the use of a kinetic thermostat can dramatically change the microscopic mechanism underlying conductivity in a molten salt.

[1] B. J. Ackerson and P. N. Pusey, Phys. Rev. Lett. **61**, 1033 (1988).

[2] J. J. Erpenbeck, Phys. Rev. Lett. **52**, 1333 (1984).

[3] D. M. Heyes, J. Chem. Phys. **85**, 997 (1997).

[4] W. Loose and S. Hess, Rheol. Acta **28**, 91 (1989).

[5] W. Loose and G. Ciccotti, Phys. Rev. A **45**, 3859 (1992).

[6] T. Yamada and S. Nosé, Phys. Rev. A **42**, 6282 (1990).

[7] W. Xue and G. S. Grest, Phys. Rev. Lett. **64**, 419 (1990).

[8] K. Bagchi, S. Balasubramian, C. J. Mundy, and M. L. Klein, J. Chem. Phys. **105**, 11183 (1996).

[9] R. A. Gray, S. Chynoweth, Y. Michopoulos, and G. S. Pawley, Europhys. Lett. **43**, 491 (1998).

[10] M. Aertsens and J. Naudts, J. Stat. Phys. **62**, 609 (1991).

[11] D. J. Evans and G. P. Morriss, *Statistical Mechanics of Nonequilibrium Liquids* (Academic Press, London, 1990).

[12] J. Dzubiella, G. P. Hoffmann, and H. Lowen, Phys. Rev. E **65**, 021402 (2002).

[13] H. Lowen and J. Dzubiella, Faraday Discuss. **123**, 99 (2003).

[14] J. Dzubiella and H. Lowen, J. Phys.: Condens. Matter **14**, 9383 (2002).

[15] J. Chakrabarti, J. Dzubiella, and H. Lowen, Phys. Rev. E **70**, 012401 (2004).

[16] O. G. Jepps and J. Petravic, Mol. Phys. **102**, 513 (2004).

[17] M. J. Stevens, M. O. Robbins, and J. F. Belak, Phys. Rev. Lett. **66**, 3004 (1991).

[18] D. Helbing, I. J. Farkas, and T. Vicsek, Phys. Rev. Lett. **84**, 1240 (2000).

[19] M. D. Haw, W. C. K. Poon, and P. N. Pusey, Phys. Rev. E **57**, 6859 (1998).

[20] M. C. Newstein, H. Wang, N. P. Balsara, A. A. Lefebvre, Y. Shnidman, H. Watanabe, K. Osaki, T. Shikata, H. Niwa, and Y. Morishima, J. Chem. Phys. **111**, 4827 (1999).

[21] B. Maranzano and N. J. Wagner, J. Chem. Phys. **117**, 10291 (2002).

[22] J. Delhommelle, J. Petravic, and D. J. Evans, Phys. Rev. E **68**, 031201 (2003).

[23] J. L. McWhirter, J. Chem. Phys. **118**, 2824 (2003).

[24] J. F. Brady, Chem. Eng. Sci. **56**, 2921 (2001).

[25] J. R. Melrose, Faraday Discuss. **123**, 355 (2003).

[26] J. Delhommelle, Eur. Phys. J. E **15**, 65 (2004).

[27] J. Delhommelle and D. J. Evans, J. Chem. Phys. **115**, 43 (2001).

[28] J. Delhommelle and D. J. Evans, J. Chem. Phys. **117**, 6016 (2002).

[29] L. Lue, O. G. Jepps, J. Delhommelle, and D. J. Evans, Mol. Phys. **100**, 2387 (2002).

[30] J. Delhommelle, J. Petravic, and D. J. Evans, J. Chem. Phys.

[31] J. Delhommelle, Phys. Rev. B **69**, 144117 (2004).

[32] J. A. Zollweg, G. V. Chester, and P. W. Leung, Phys. Rev. B **39**, 9518 (1989).

[33] J. A. Zollweg and G. V. Chester, Phys. Rev. B **46**, 11186 (1992).

[34] J. Q. Broughton, G. H. Gilmer, and J. D. Weeks, Phys. Rev. B **25**, 4651 (1982).

[35] K. Bagchi, H. C. Andersen, and W. Swope, Phys. Rev. E **53**, 3794 (1996).

[36] J. Petravic and J. Delhommelle, J. Chem. Phys. **118**, 7477 (2003).

[37] H. H. Rugh, Phys. Rev. Lett. **78**, 772 (1997).

[38] O. G. Jepps, G. Ayton, and D. J. Evans, Phys. Rev. E **62**, 4757 (2000).

[39] W. K. den Otter and J. H. R. Clarke, Europhys. Lett. **53**, 426 (2001).

[40] P. Nikunen, M. Kartunnen, and I. Vattulainen, Comput. Phys. Commun. **153**, 407 (2003).

[41] T. Soddemann, B. Dunweg, and K. Kremer, Phys. Rev. E **68**, 046702 (2003).

[42] G. F. Voronoi, J. Reine Angew. Math. **28**, 91 (1908).

[43] S. Hess, Physica A **240**, 126 (1997).

[44] S. Hess, Int. J. Thermophys. **23**, 905 (2002).

[45] D. J. Evans and G. P. Morriss, Phys. Rev. Lett. **56**, 2172 (1986).

[46] P. Padilla and S. Toxvaerd, J. Chem. Phys. **103**, 716 (1995).

[47] K. P. Travis, P. J. Daivis, and D. J. Evans, J. Chem. Phys. **105**, 3893 (1996).

[48] J. Delhommelle, J. Petravic, and D. J. Evans, J. Chem. Phys. **120**, 6117 (2004).

[49] J. Delhommelle and J. Petravic, J. Chem. Phys. **118**, 2783 (2003).

[50] J. Petravic and J. Delhommelle, J. Chem. Phys. **119**, 8511 (2003).

119, 11 005 (2003).